Physical Properties of DNA and Chromatin Isolated from G_1- and S-Phase HeLa S-3 Cells. Effects of Histone H1 Phosphorylation and Stage-Specific Nonhistone Chromosomal Proteins on the Molar Ellipticity of Native and Reconstituted Nucleoproteins during Thermal Denaturation†

Thomas W. Dolby, Kozo Ajiro, Thaddeus W. Borun,‡ R. Stewart Gilmour, Alfred Zweidler, Leonard Cohen, Paul Miller, and Claudio Nicolini*

ABSTRACT: To help delineate how changes in chromatin organization are related to DNA replication and transcription during the HeLa S-3 cell cycle, we have extended previous studies of the composition and structure of chromatin in synchronized G_1- and S-phase cells. By analyzing changes in molar ellipticity at 276 nm ($[\theta_{276}]$) during thermal denaturation, it was found that double-helical DNA molecules in native chromatin have different optical activities and thermal stabilities at these two stages of the cell cycle. Furthermore, profiles of $d[\theta_{276}]/dT$ vs. T indicate that native G_1- and S-phase chromatins contain different families of DNA superstructures. To help determine the causes and functional significance of these chromatin reorganizations during the cell cycle, we compared the optical activities and thermal stabilities of DNA in native chromatin with protein-free DNA and DNA in nucleoproteins reconstituted in vitro by NaCl–urea gradient dialysis. In addition, we examined levels of histone phosphorylation, histone acetylation, and types of histone and nonhistone chromosomal proteins (NHCP) found in G_1- and S-phase cells and in purified hydroxylapatite (HAP) fractions of these nuclear proteins which were used for in vitro reconstitution. The results of the present studies indicate that changes in H1–DNA–NHCP interactions occur in vivo, are associated with the phosphorylation of histone 1 molecules, and appear to be responsible for the relaxation of compact G_1-phase chromatin superstructures into more open S-phase configurations during the HeLa S-3 cell cycle.

Recent physical studies by use of a variety of techniques have demonstrated that most regions of the large double-helical nuclear DNA molecules in eucaryotic cells are associated with chromosomal proteins and are organized into more or less compact nucleoprotein superstructures. Thus, when examined in situ (Weintraub & Groudine 1976; Kendall et al., 1977) and in native chromatin preparations (Olins & Olins 1974; Nicolini & Baserga, 1975; Oudet et al., 1975; Woodcock et al., 1976; Kornberg, 1977), eucaryotic nucleoproteins are generally found organized in a hierarchy of configurations ranging from the nucleosome, which is a simple element of DNA superstructure, to highly complex and possibly functionally specific types of polynucleosomal folds, coils, and supercoils.

Although there are indications that reorganizations in these chromatin superstructures reflect the regulation of DNA replication (Nicolini et al., 1975; Kendall et al., 1977) and transcription in many different types of eucaryotic cells (Seligy & Lurquin, 1973; Polacow & Simpson, 1973; Gottesfeld et al., 1975; Garel et al., 1977; Weintraub & Groudine, 1976; Baserga & Nicolini, 1976), the specific changes in chromatin organization associated with each of these DNA copying processes and their control have not yet been clearly determined in a single experimental system. For example, in the first of our previous studies of chromatin structural changes during the HeLA S-3 cell cycle, measurements of CD[1] between 250 and 300 nm indicated that maximum positive values of molar ellipticity [θ] were lowest during mitosis when neither replication nor transcription occurs at appreciable rates, increased somewhat during the G_1 phase when transcription is resumed and, reached maximal levels during the S-phase (Nicolini et al., 1975) when both replication and transcription occur at their highest rates. Since molar ellipticity signals between 260 and 280 nm are thought to be generated by asymmetric arrangements of chiral chromophores in double-helical DNA molecules (Fasman et al., 1964; Shih & Fasman, 1972; Bayley, 1973) and it has been shown that these optical signals can be significantly modified by subtle changes in base tilting and electromagnetic interactions between neighboring nucleotide moieties (Cech et al., 1976), it appeared that a rigorous structural interpretation of these preliminary findings would be difficult.

In a subsequent study, however, evidence concerning the type of physical changes responsible for our initial molar ellipticity observations was obtained by use of quantitative nuclear morphometry (Kendall et al., 1977). These morphometric analyses demonstrated that HeLa chromatin condensed somewhat during the course of the phase G_1 and then abruptly assumed its most disperse configurations during the S phase. Thus, complementary results obtained in two different kinds of structural studies indicate that increases in

† From the Wistar Institute of Anatomy and Biology, Philadelphia, Pennsylvania 19104 (T.W.D., K.A., and T.W.B.), The Beatson Institute, Glasgow, Scotland (R.S.G.), the Institute for Cancer Research, Fox Chase Cancer Center, Philadelphia, Pennsylvania 19111 (A.Z. and L.C.), and the Division of Biophysics, Temple University Health Sciences Center, Philadelphia Pennsylvania 19140 (P.M. and C.N.) *Received May 31, 1978; revised manuscript received October 20, 1978.* Supported by U.S. Public Health Service Research Grants CA 11463, CA 12923, CA 12544, CA 15135, CA 17856, CA 18258, and CA 20034 from the National Cancer Institute. We dedicate this paper to the memory of Dr. Thaddeus Borun, who suddenly died January 1979.

‡ Recipient of Career Development Award CA 00088 from the National Cancer Institute. Deceased January 1979.

[1] Abbreviations used: TPCK, L-1-tosylamide-2-phenylethylchloromethyl ketone; TLCK, *N*-α-*p*-tosyl-L-lysine chloromethyl ketone hydrochloride; PMSF, phenylmethanesulfonyl fluoride; HAP, hydroxylapatite; CD, circular dichroism; NHCP, nonhistone chromosomal proteins; EDTA, ethylenediaminetetraacetic acid; *A*, absorbance.

0006-2960/79/0418-1333$01.00/0

positive values of chromatin molar ellipticity [Θ_{276}] during the G_1–S transition of the HeLa cell reflect and are probably caused by the reorganization of compact G_1 DNA superstructures into disperse S-phase configurations. Similar continuous changes in chromatin superstructures through the cell cycle have been also shown by cell fusion experiments (Rao et al., 1976).

Previous studies (Miller et al., 1976; Tashiro & Kurokawa, 1975) have shown that molar ellipticity sensitively reflects the changes in chromatin conformation which occur during denaturation.

In the present paper we describe the results of studies that indicate that parameters derived from molar ellipticity measurements during thermal denaturation can detect structural differences between native G_1- and S-phase chromatin and reconstituted nucleoproteins. In addition, these techniques prove to be useful for comparing the structures of nucleoproteins formed during gradient dialysis of DNA with various combinations of G_1- and S-phase histone and NHCP. Such comparisons were then used to assess the effects of components in stage-specific histone and NHCP fractions on the structure, thermal stability, and function of native and reconstituted chromatin.

Experimental Procedures

Materials

Joklik-modified Eagle's minimal essential spinner medium, minimal essential medium, Earle's balanced spinner salt solution, and fetal calf and calf serum were obtained from Grand Island Biological Co. AG-501-X8(D) mixed-bed resin was purchased from Bio-Rad. HAP was prepared and recrystallized as previously described (MacGillivray et al., 1972). [2-^{14}C]Thymidine (58.9 Ci/mol) and all other radioisotopes were obtained from New England Nuclear. Proteinase K was obtained from Merck, Darmstadt, West Germany. All other reagents were purchased from Sigma Chemical Co.

Methods

(*a*) *Cell Culture and Synchronization.* Logarithmically growing HeLa S-3 cells were maintained in suspension culture at 37 °C at concentrations of between 2×10^5 and 5×10^5 cells/mL in Joklik-modified Eagle's minimal essential spinner medium supplemented with 3.5% each (v/v) fetal calf and calf serum.

The basic procedure for selective detachment of mitotic cells on a small scale has been published by Terasima & Tolmach (1963) and Robbins & Marcus (1964). The labeling index (LI) and mitotic rate (MR) were determined by autoradiography (Nicolini et al., 1975), on aliquots of cells at various time intervals after selective detachment: at $t = 0$ h, about 90% of the cells are in mitosis; at $t = 3.0$ h with LI = 5% and MR = 3%, about 90% of the cells are in "G_1 phase"; at $t =$ 11 h, the cells are at the peak of DNA synthesis with LI = 83% and MR = 1% ("S phase"). At later times after mitosis, the degree of synchrony is markedly reduced (Nicolini et al., 1975), even though a large number of cells are in the G_2 phase between 14 and 18 h. Large quantities of selectively detached synchronized HeLa S-3 cells were prepared as described (Borun et al., 1975).

In each experiment the total yield of M-phase cells was about (3–4) $\times 10^5$ cells/mL in a final volume of 1800 mL. Ninety to ninety-five percent of the cells was found to be in mitosis by phase-contrast microscopy. The cells were maintained in suspension culture and harvested as indicated below.

(*b*) *Radioisotope Labeling.* Relative rates of DNA replication at various times after selective detachment were determined by pulse labeling 2 mL of synchronized culture with 0.2 μCi of [^{14}C]thymidine for 30 min at 37 °C, followed by Cl_3AcOH precipitation on Millipore filters and scintillation counting of Cl_3AcOH-precipitable material as previously described (Marks et al., 1973).

To detect ^{32}P-labeled phosphorylated histone species, 200 mL of log-phase cultures at 5×10^6 cells/mL were incubated in phosphate-free spinner medium with 20–100 μCi of [^{32}P]orthophosphate for 3 h, followed by histone extraction as previously described (Marks et al., 1973).

To detect [^{3}H]acetate-labeled histone species, 200-mL of log-phase cultures of cells at 5×10^6 cell/mL were incubated with 200–500 μCi of [^{3}H]acetate and 100 μg/mL of cycloheximide for 1 h. In control cultures, cycloheximide was omitted. Comparisons of histone species labeled both in the presence and absence of cycloheximide were used to determine which species were acetylated and which were incorporating [^{3}H]acetate in the form of amino acids derived from acetate. Histones were extracted from the labeled cells as previously described (Marks et al., 1973).

(*c*) *Isolation of High Molecular Weight DNA from HeLa S-3 Cells.* Previous studies (R. S. Gilmour, unpublished observations) have shown that functionally active reconstituted chromatin (Gilmour et al., 1975) can be obtained only if high molecular weight DNA is used during reconstitution. High molecular weight DNA was therefore isolated from log-, G_1-, and S-phase HeLa cells as described below and used in all studies reported here.

Approximately 600 mL of G_1 (3-h postmitosis) or S (11-h postmitosis) phase synchronized HeLa S-3 cells (3×10^5 cells/mL) were harvested by centrifugation (approximately 600*g* for 5 min at 37 °C). The cell pellets were washed twice by resuspensions in 40 mL of ice-cold spinnner salts and recovered between washings by centrifugation at approximately 1000*g* for 3 min at 4 °C. The washed cell pellets were resuspended in 20 mL of cold hypotonic buffer (10 mM Tris-HCl, 10 mM KCl, 1.5 mM $MgCl_2$), pH 7.4, and allowed to swell on ice for 7–9 min. The swollen cells were homogenized in a stainless steel Dounce homogenizer (0.001-in. clearance) and the homogenate was centrifuged (2000*g* for 10 min) at 4 °C to yield a nuclear pellet. Log-phase nuclei were similarly prepared by use of 10 times more starting material.

Starting with 2×10^6 nuclei/mL resuspended in 10 mM Tris-HCl (pH 8.0), 10 mM EDTA, 10 mM NaCl, 0.5% sodium dodecyl sulfate, 50 μg/mL of proteinase K, the nuclei were subjected to the procedure used by Gross-Bellard et al. (1973) to isolate high molecular weight DNA. Log-phase HeLa DNA was stored at 0.5 mg/mL at −20 °C until it was used for reconstitution. G_1- and S-phase DNA were finally dialyzed overnight against 0.7 mM sodium phosphate buffer (pH 6.8) and used immediately thereafter at a concentration of about 0.5 A_{260}/mL for analysis of molar ellipticity, [Θ_{276}], during thermal denaturation.

Estimations of molecular weight were made by observation of the sedimentation rates of sonicated and unsonicated DNA samples in 5–20% alkaline sucrose gradients in an SW27 rotor (2.7×10^4 rpm) for 70 min at 5 °C in a Beckman L2-65B ultracentrifuge by use of several DNA dilutions (1–15 μg/gradient). The DNA markers and procedures used were in accordance with those outlined by Parodi et al. (1975) and by Cox et al. (1973). Molecular weight was estimated by use

of a regression equation based on the molecular weights of T4 and T7 phage and SV40 DNA (Parodi et al., 1975) vs. elution volume (log molecular weight = 2.379 log [elution volume (mL)] + 5.64).

All samples of unsonicated DNA were homogeneous and had apparent single-stranded molecular weights $\geq 1.9 \times 10^9$ given the limitations of the method (Ormerod & Lehmann, 1971; van der Schans et al., 1969; Eijher et al., 1962). Any extensive DNA strand breakage during isolation producing lower molecular weights could have been detected, since briefly sonicated S-phase DNA was found distributed in three principal molecular weight classes in these alkaline sucrose gradients.

(*d*) *Isolation of Native Chromatin.* Nuclei were isolated (as described in the preceding section of these Methods) from selectively detached cells in either G_1 (3-h postmitosis) or S (11-h postmitosis) phase up to and including homogenization of swollen cells. At that point 0.25 volume (v/v) of 1 M sucrose (cold) was added to the homogenate and thoroughly mixed by gentle homogenization. The homogenate was then centrifuged at 2000*g* for 10 min at 4 °C. The resulting nuclear pellet was resuspended by gentle homogenization in 20 mL of a solution of 2.2 M sucrose, 1 mM $MgCl_2$, and 0.1 mM dithiothreitol, pH 7.4, and centrifuged at 30000*g* for 1 h at 4 °C. The nuclei were resuspended in a 20-mL solution containing 10 mM Tris-HCl, 10 mM KCl, 1.5 mM $MgCl_2$, pH 7.4, and 1% Triton X-100 and recentrifuged at 12000*g* for 10 min at 4 °C. The pellet was resuspended in 20 mL of 0.14 M NaCl, pH 7.4, and recentrifuged at 12000*g* for 10 min in aliquots to obtain chromatin pellets. CD studies with soluble native chromatins were conducted immediately by suspending selected chromatin pellets in 0.7 mM sodium phosphate buffer (pH 6.8) to a concentration of 0.5–1 A_{260}/mL.

(*e*) *Fractionation of Chromosomal Proteins.* The procedure used was similar to that described by MacGillivray et al. (1972). Chromatin pellets were resuspended by homogenization in 5 mL of ice-cold 2 M NaCl, 4 M urea [previously passed through a 5 × 60 cm column of Bio-Rad 501-XS(D) resin], 1 mM dithiothreitol, 0.1 mM TPCK, TLCK, 1 mM PMSF, and 1 mM sodium phosphate, pH 6.0. The solution was sonicated on ice 10 times at 50 W for 3 s each time. An aliquot was diluted to 1:100 in 0.1 M NaOH and the total A_{260} calculated (approximately 60 A_{260} = approximately 3.2 mg of DNA).

The sonicated and dissociated chromatin was applied to a 2 × 10 cm HAP column that had been previously equilibrated with a solution of 2 M NaCl, 4 M urea (deionized), 1 mM dithiothreitol, 1 mM sodium phosphate, pH 6.0 at 25 °C. The column was eluted with the equilibration buffer and 5-mL fractions were collected until the A_{280} of the eluent was <0.02. Fractions containing significant A_{280} were pooled to yield approximately 20 mL of histone fraction. Histone fractions were adjusted to 0.1 mM PMSF and stored at 4 °C until they were reconstituted. Nonhistone proteins and some of the nuclear RNA were eluted with a solution of 0.2 M sodium phosphate, 2 M NaCl, 4 M urea, 1 mM dithiothreitol, pH 6.0 (yield is approximately 15 mL). Finally, double-stranded DNA and the remainder of the nuclear RNA were eluted with 0.5 M sodium phosphate, 2 M NaCl, 4 M urea, 1 mM dithiothreitol, pH 6.0. Total recovery of nucleic acids was approximately 90% and protein was 93% based on spectrophotometric measurements.

Since the HAP nonhistone protein fraction contains significant quantities of RNA, an equal volume of 55% CsCl, 4 M urea, 50 mM sodium phosphate, 1 mM PMSF, 1 mM dithiothreitol, 1 mM EDTA (pH 6.0) was mixed with the pooled nonhistone fractions and centrifuged with an overlay of mineral oil at 40000 rpm for 40 h at 10 °C in a Beckman L2-65B in a 50 Ti fixed-angle rotor. After centrifugation, the upper three-fourths of the aqueous CsCl gradients generated by centrifugation were pooled and found to contain the nonhistone proteins, while the pellet and lower fourth of the gradient were found to contain RNA.

(*f*) *Analysis of HAP Histone and Nonhistone Fractions by Electrophoresis on Polyacrylamide Slab Gels Containing Triton X-100.* Samples of the fractions obtained by chromatography on HAP were diluted 1:6 with deionized H_2O, and 120% (w/v) Cl_3AcOH was added to a final concentration of 20%. The proteins precipitated at 3 °C overnight were collected by centrifugation at 17000*g* for 10 min at 3 °C. The pellets were washed once with 5 mL of acetone–0.2% HCl and twice with 5 mL of acetone and resuspended in a small volume (50–100 μL) of deionized H_2O. After reading the absorbance at 280 nm, the samples were diluted to a final concentration of 1.5 mg/mL with sample buffer (8 M urea, 10% mercaptoethanol, 0.02% pyronin Y), and 12–30 μg of protein was resolved by electrophoresis at 120 V for 15 h as previously described (Borun et al., 1977) on 14 × 30 cm polyacrylamide slab gels which were 0.75-mm thick. After staining with Amido Black and electrical destaining (Borun et al., 1977), the slab gels were scanned at 600 nm by use of a Gilman ACD-15 spectrophotometer.

(*g*) *Determination of Histone Phosphorylation and Acetylation Levels during the HeLa S-3 Cell Cycle.* At various times after selective detachment, 100-mL samples containing 5×10^5 cells/mL were harvested and washed three times with 50 mL of ice-cold spinner salts (Earle's balanced salt solution), followed by centrifugation at 600*g* for 5 min at 3 °C between washings. Nuclei were prepared by washing three times with 25 mL of ice-cold 80 mM NaCl, 20 mM EDTA, 1% Triton X-100, and twice with 25 mL of ice-cold 0.15 M NaCl by resuspension and centrifugation as above. Nuclear pellets were then frozen at −20 °C until all samples had been collected. Histones were prepared by the method of Zweidler (unpublished experiments). Nuclear pellets were thawed, resuspended in 2 mL of 2 M NaCl, 10 mM EDTA, pH 7.2, and homogenized thoroughly in a micro Dounce homogenizer. After centrifugation at 40000*g* for 15 min at 3 °C to remove insoluble material, DNA was precipitated from the supernatant homogenate by the addition of HCl to a final concentration of 0.25 N. After centrifugation at 5000*g* for 10 min at 3 °C, this supernatant was removed and brought to a final concentration of 20% Cl_3AcOH by the addition of one-fifth volume of 120% Cl_3AcOH (1.2 g of Cl_3AcOH/mL) and chilled for 30 min at 3 °C. After centrifugation at 10000*g* for 10 min the pelleted histones were washed once with 20 volumes of 20% Cl_3AcOH_3 once with 20 volumes of acetone–0.2% HCl, and three times with 20 volumes of acetone at 3 °C. After resuspension to a concentration of 1 mg/mL in 10 mM HCl, histones other than H1 were precipitated by the addition of an equal volume of 10% Cl_3AcOH and chilled for 30 min on ice. After centrifugation at 10000*g* for 10 min at 3 °C, the pelleted nucleosomal core histone fraction was washed with acetone–0.2% HCl and acetone as above. Histone H1 was precipitated from the 5% Cl_3AcOH supernatant by the addition of Cl_3AcOH to a final concentration of 20% and chilled for 30 min on ice, followed by centrifugation. The H1 pellet was then washed with acetone–HCl and acetone as

above, and all fractions were resuspended to a concentration of about 1 mg/mL in sample buffer as previously described (Methods section f) (Borun et al., 1977). Various phosphorylated and acetylated histone species in these fractions were resolved by electrophoresis of 20 μg of protein at 200 V for 24 h on 28-cm long × 4-mm diameter polyacrylamide gels containing 6 M urea and 6 mM Triton X-100 as previously described (Borun et al., 1975, 1977; Zweidler & Borun, 1974). Fractions labeled a in Figure 3 were identified by the fact that these species incorporated [^{3}H]acetate both in the presence and absence of 100 mM cycloheximide (Methods section b). Fractions labeled "p" were identified by the fact that ^{32}P was incorporated into these species during ^{32}P labeling (Methods section b). Relative levels of different acetylated and phosphorylated histones were determined by integrating the areas under each of the indicated peaks on tracings of stained gels and dividing the area of each of the modified species by the total area of all histone species of that type.

(*h*) *Nucleoprotein Reconstitution from High Molecular Weight DNA and Chromosomal Protein Fractions.* HeLa log-phase high molecular weight DNA and either G_1- or S-phase histone or nonhistone chromosomal proteins isolated by HAP chromatography were mixed to yield the same A_{280} (histone and nonhistone protein) to A_{260} (DNA) ratio as native G_1- or S-phase chromatins [0.073 and 0.075, respectively, i.e., [S(H)S(NH)] = (0.7 A_{280} of HAP histones + 0.35 A_{280} of HAP NHCP)/(1.4 A_{260} of DNA)]. The mixture was dialyzed against 100 volumes of 0.5 M NaCl, 4 M urea (deionized), 50 mM sodium phosphate, 1 mM dithiothreitol, 0.1 mM PMSF (pH 6.0), overnight at 4 °C, followed by a change of the external medium to 0.14 M NaCl alone. Dialysis was continued for 5 h at 4 °C. The reconstituted chromatin precipitate was recovered by centrifugation at 12000*g* for 10 min at 4 °C. The undiluted supernatant was scanned from 360 to 200 nm to detect uncomplexed nucleic acid or protein. The A_{260} and A_{280} were found to be less than 0.03 or 0.2% of total. The pellet of the reconstituted complex was immediately resuspended in 0.7 mM sodium phosphate (pH 6.8) to a concentration of 0.5–1 A_{260}/mL and analyzed by measurement of $[\Theta_{276}]$ during thermal denaturation.

(*i*) *Molar Ellipticity Measurements of DNA, Chromatin and RNA during Thermal Denaturation.* Circular dichroism measurements were performed with a Jasco Model J40 recording spectropolarimeter equipped with CD. The sample temperature was altered at 1 °C/min by pumping solvent through the water-jacketed fused quartz cell from a HETO circulating bath equipped with a PG-UL thermostat. The sample temperature was continuously monitored with a Bailey thermocouple at the jacket exit. Absorbance and ellipticity at 276 nm were recorded simultaneously. Molar ellipticity, $[\Theta]$, is defined as ±deg cm^2/dmol of nucleotide residue. The assumed mean residue molecular weight is 330. The instrument was calibrated and operated under conditions previously reported (Nicolini & Baserga, 1975; Nicolini et al., 1976). CD and absorbance measurements were corrected for light-scattering artifacts as previously described (Nicolini et al., 1976; Nicolini & Kendall, 1977).

(*j*) *Plots of the Derivatives of Absorbance and Molar Ellipticity vs. Temperature.* Plots of the derivatives of $[\Theta_{276}]$ and A_{276} vs. temperature were constructed with a CDC 6400 computer, by use of an algorithm that allowed precise determination of the transition points during denaturation and renaturation of chromatins and DNA. The n data points, equally spaced at intervals of h = 0.1 °C, were arranged in order of ascending temperature. A least-squares parabola (T) = $Q_0 + Q_1T_1 + Q_2T_2^2$ was first fitted through the first five points (K = 1, 2, ..., 5) and then differentiated to evaluate the derivative at the middle point (3), where any fitted polynomial estimates the true underlying function with the greatest accuracy (Milgram, 1975), specifically $d[\Theta_{276}]/dT_{T=K} = (1/10h)(-2\Theta_{K-2} - \Theta_{K-1} + \Theta_{K+1} + 2\Theta_{K+2})$. Next, we grouped together points 2–6, determined the least-squares parabola through these five points, and again evaluated the derivative at the middle point (4). The procedure is iterated, including grouping of points (n − 4), (n − 3), (n − 2), (n − 1), and n. This will yield an estimate of the value of the derivative $d[\Theta_{276}]/dT$ (or dA_{276}/dT) at points 3, 4, ..., (n − 2) (i.e., every 0.1 °C in the explored temperature range 3–92 °C). For the first and last two temperature points, we group respectively the first and last five points, find the least-squares quadratic, differentiate, and evaluate the derivative at 1, 2, (n − 1), and n temperature points. This approach has several advantages. (1) It is "model free"; that is, we did not need a thermodynamic model that has the ability to approximate the data throughout its entire range. (2) Erratic data points due to noise will influence only a few points on the derivative plot, whereas if the entire set of data were fitted and differentiated, these errors would be propagated throughout the entire range. Since values of $[\Theta_{276}]$ at temperatures between 3 and 30 °C were invariant, this temperature interval has been deleted from the various figures. Values of $[\Theta_{276}]$ were corrected for differential light-scattering artifacts before calculating $d[\Theta_{276}]/dT$ vs. T plots (Nicolini & Kendall, 1977).

Results

(*1*) *Analysis of Differences in the Superstructural Organization of DNA in Native G_1- and S-Phase Chromatin by Use of Measurements of Molar Ellipticity during Thermal Denaturation.* (*A*) $[\Theta_{276}]^{27°C}$ *of Protein-Free DNA and Native Chromatin Isolated from Synchronized G_1- and S-Phase HeLa S-3 Cells.* Preliminary CD studies have shown that the molar ellipticity of isolated chromatin increases as HeLa cells pass from G_1 into S phase (Nicolini et al., 1975). To determine if this increase could be caused by differences in the intrinsic optical properties of G_1- and S-phase DNA molecules, the initial molar ellipticities of DNA chromatin isolated from G_1- and S-phase cells were measured at 27 °C, prior to thermal denaturation. The values of $[\Theta_{276}]^{27°C}$ are shown in Table I and indicate the following.

(a) Protein-free, high molecular weight G_1- and S-phase DNA have similar, high positive molar ellipticities in solution ($[\Theta_{276}]^{27°C}$ = 7600–7700 deg cm^2/dmol) which are also similar to the $[\Theta_{276}]^{27°C}$ of DNA isolated from log-phase cells (data not shown). Thus, the inherent optical asymmetry of DNA molecules does not appear to change significantly during the HeLa cell cycle, as expected.

(b) The $[\Theta_{276}]$ of isolated G_1-, S-, and log-phase DNA contain no detectable differential light-scattering components. In contrast, native chromatins and reconstituted nucleoproteins were found to scatter different amounts of left- and right-handed, circularly polarized light during CD measurements. Therefore, all values of chromatin and nucleoprotein molar ellipticity determined in this study were corrected as described by Nicolini & Kendall (1977) to compensate for these significant light-scattering artifacts. Typical corrections are shown in Table I.

(c) Confirming previous observations (Nicolini et al., 1975), the corrected $[\Theta_{276}]^{27°C}$ of DNA in native HeLa chromatin

Table I: Parameters Derived from Molar Ellipticity Measurements during Thermal Denaturation of DNA, Native Chromatin, and Reconstituted Nucleoproteins[a]

	uncorrected $[\Theta_{276}]^{27\,°C}$ (deg cm²/dmol)	differential light-scattering component $[\Theta_{276}]^{27\,°C}$ (deg cm²/dmol)	corrected $[\Theta_{276}]^{27\,°C}$ (deg cm²/dmol)	corrected $[\Theta_{276}]^{max}$ (deg cm²/dmol)	$\Delta[\Theta_{276}]$ (deg cm²/dmol)	$T_{\Theta initial}$ (°C)	ΔT (°C)	$T_{\Theta max}$ (°C)	$\Delta[\Theta_{276}]/\Delta T$ [(deg cm²/dmol)/°C]	T_m (°C)
protein-free DNA: G_1 DNA	7600	0	7600	7600	0					57
S DNA	7700	0	7700	7700	0					55
native chromatin: G_1 native	4550	750	3800	6980	3180	46	43	89	74	>92
S native	5500	394	5106	7158	2052	48	23	71	89	82
reconstituted nucleoproteins										
homologous components										
$G_1(H)G_1(NH)$	4500	669	3831	7204	3373	52	28	80	121	86
S(H)S(NH)	4300	900	3400	6400	3000	49	34	83	88	88
hybrid components										
$G_1(H)S(NH)$	4400	1329	3071	6650	3597	58	23	81	156	90
$S(H)G_1(NH)$	4212	1206	3006	7842	4836	54	23	77	210	92
reconstituted nucleolistone										
$G_1(H)$	5400	313	5087	7704	2617	55	17	72	154	80
S(H)	4600	846	3754	7531	3777	47	34	81	111	86

[a] Samples were prepared and suspended in 0.7 mM sodium phosphate buffer, pH 6.8. for subsequent CD measurements as described under Methods and Table II. Uncorrected $[\Theta_{276}]^{27\,°C}$ is the observed molar ellipticity at 27 °C prior to differential light-scattering corrections (deg cm²/dmol). Corrected $[\Theta_{276}]^{27\,°C}$ is the light-scattering corrected (Nicolini & Kendall, 1977) molar ellipticity (deg cm²/dmol) at 27 °C. $\Delta[\Theta_{276}]$ (deg cm²/dmol) is the difference between corrected $[\Theta_{276}]^{max}$, the maximum positive $[\Theta_{276}]$ observed during thermal denaturation, and $[\Theta_{276}]^{27\,°C}$. $T_{\Theta initial}$ is the temperature (°C) at which positive changes in $[\Theta_{276}]$ begin and $T_{\Theta max}$, the temperature (°C) at which $[\Theta_{276}]^{max}$ is observed. ΔT (°C) represents the difference between $T_{\Theta max}$ and $T_{\Theta initial}$. The dimensions of $\Delta[\Theta_{276}]/\Delta T$ are (deg cm²/dmol)/°C. T_m (°C) is the temperature at which 50% of DNA double helixes have melted into random coils.

increases from 3800 deg cm²/dmol in mid-G_1 to 5106 deg cm²/dmol in mid-S phase.

Since the $[\Theta_{276}]^{27°C}$ values of protein-free G_1- and S-phase DNA are similar to each other, it is evident that the substantial increase in native chromatin $[\Theta_{276}]^{27°C}$, which occurs as cells pass from G_1 into S phase, must reflect changes in DNA conformation induced by the reorganization of nucleoprotein superstructures. The type of structural reorganization responsible for these increases in the ellipticity of native chromatin is indicated by the results of quantitative morphometric studies of HeLa cell nuclei, stained in situ with Azure B (Kendall et al., 1977), which have shown that compact chromatin configurations found in late G_1-phase cells abruptly become more disperse during the S phase. When considered together, all of the preceding observations indicate that DNA molecules in native G_1- and S-phase chromatin are less optically active and more physically superpacked than protein-free HeLa DNA in solution, and they also demonstrate that the magnitude of $[\Theta_{276}]^{27°C}$ increases as DNA configurations in native chromatin become more physically disperse. It is therefore reasonable to conclude from these data that increases in native chromatin $[\Theta_{276}]^{27°C}$ found at the transition from G_1 into S phase reflect the relaxation of DNA molecules in compact G_1-phase configurations and the formation of more disperse S-phase organizations during the HeLa cell cycle.

(*B*) *DNA and Native Chromatin T_m Determinations from Profiles of $d[\Theta_{276}]/dT$ vs. T.* In previous studies (Augenlicht et al., 1974; Parodi et al., 1975; Mandel & Fasman, 1974, 1976), decreases in molar ellipticity were compared with hyperchromicity during the thermal denaturation of protein-free DNA. In these studies it was shown that T_m, the temperature at which 50% of double-stranded DNA helixes has melted into hyperchromatic single-stranded random-coil configurations, was the temperature at which $d[\Theta_{276}]/dT$ reaches its maximum negative value in profiles of $d[\Theta_{276}]/dT$ vs. T. By use of this precise method of determining T_m during thermal denaturation, we found the following.

(a) Protein-free G_1- and S-phase double-stranded DNA helixes begin melting at nearly the same temperature (G_1, 50 °C; S, 49 °C) and exhibit similar decreases in $d[\Theta_{276}]/dT$ (Figure 1 and Table I).

(b) G_1-phase DNA is only slightly more stable than S-phase DNA at temperatures lower than T_m.

(c) The T_m of G_1-phase DNA (57 °C) is only slightly higher than the T_m of S-phase DNA (55 °C).

(d) At temperatures greater than T_m, similar small negative inflections can be seen in the $d[\Theta_{276}]/dT$ vs. T profiles of G_1- and S-phase DNA in Figure 1a. [It should be noted here that the underlying structural changes generating these "thermolytes" during denaturation (Ansevin et al., 1976) have not been firmly established since, in contrast to T_m values, which are not significantly affected by variations in mathematical procedure, the position and magnitude of these minor negative inflections are altered by changes in the algorithm used to transform $[\Theta_{276}]$ vs. T or hyperchromicity vs. T profiles into their derivative values.]

(e) The overall thermal stabilities and T_m of protein-free G_1- and S-phase DNA are not only essentially similar to each other but are also similar to the stability and T_m of high molecular weight DNA isolated from log-phase HeLa cells (data not shown). Thus the inherent thermal stability of HeLa DNA does not appear to change significantly during the cell cycle.

When these results are compared with the negative components of the chromatin $d[\Theta_{276}]/dT$ vs. T profiles in Figure

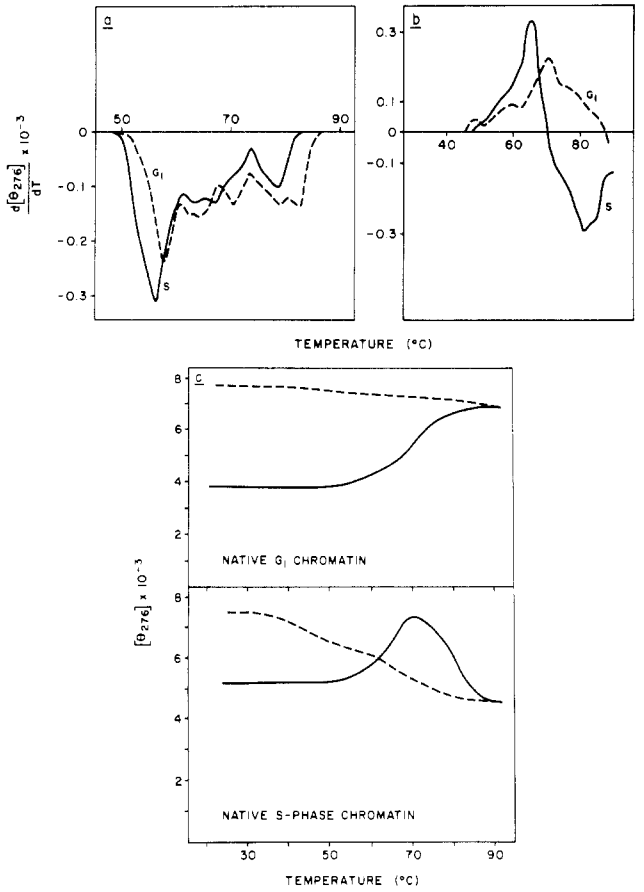

FIGURE 1: (a) Temperature dependence of the first derivative ($d[\Theta]/dT$) of molar ellipticity at 276 nm of high molecular weight DNA isolated from G_1- (---) and S-phase (—) synchronized HeLa S-3 cells. Light-scattering corrected molar ellipticity measurements observed during thermal denaturation of DNA were transformed to this derivative form as described in the Methods section. The solvent was 0.7 mM sodium phosphate, pH 6.8. $d[\Theta]/dT$ is expressed in (deg cm^2/dmol)/°C × 10^{-3}. The maximum negative inflection corresponds to T_m of the DNAs. (b) Temperature dependence of the first derivative ($d[\Theta]/dT$) of molar ellipticity at 276 nm of native chromatin isolated from G_1- (---) and S-phase (—) synchronized HeLa S-3 cells. $d[\Theta_{276}]/dT$ minima represent T_m. The solvent was 0.7 mM sodium phosphate, pH 6.8. $d[\Theta_{276}]/dT$ is expressed in (deg cm^2/dmol)/°C × 10^{-3}. (c) Changes in molar ellipticity at 276 nm during thermal denaturation (—) and renaturation (---) of native G_1- and native S-phase HeLa S-3 chromatin, as described in Figure 1b.

1b and data in Table I, it can be seen that the T_m of DNA in native chromatins is 20–30 °C higher than the T_m of protein-free G_1- and S-phase DNA. Furthermore, the T_m of double-helical DNA in G_1-phase chromatin (>92 °C) is at least 10 °C higher than the T_m of DNA in S-phase chromatin (82 °C).

Such T_m assignment is justified also in the ground of previous work (Miller et al., 1976; Nicolini, 1979; Fasman, 1979), where, even in native chromatin, only the helix–coil transition is characterized by a substantially decreased signal and a red shift in the 250–300 nm CD spectra.

Furthermore, renaturation studies show (Miller et al., 1976; Nicolini, 1979) that even in chromatin from G_1 and S phase (Figure 1c) the transition accompanied by a *decreased* molar ellipticity is *reversible*, while the transition accompanied by an *increased* molar ellipticity is *irreversible*, likely because chromosomal proteins are irreversibly denaturated and consequently their electrostatic interactions with DNA phosphate (responsible for the higher order structure) are *irreversibly* destroyed (Miller et al., 1976; Wilhelm et al., 1974).

The similar high $[\Theta_{276}]$ values ultimately reached during the renaturation of denatured G_1- and S-phase chromatin indeed suggest that chromosomal proteins, which are irreversibly changed by heating to 92 °C, were initially responsible for different DNA organization in native chromatin, since optically asymmetric double-helical DNA molecules are not reorganized into lower $[\Theta_{276}]$ configurations after these proteins have been denatured. The separation between helix–coil transition (negative maximum in the derivative, i.e, T_m) and superhelix–helix transition (several positive maxima in the derivative, T_{S-H}) has been previously shown (Miller et al., 1976; Fasman, 1979; Wilhelm et al., 1974) to be achievable only by CD measurement in native chromatin (not by absorbance where several peaks of similar sign can be observed in the absorption derivative).

Considering that even the nucleosome superstructure shows positive maxima in the $d\Theta/dT$ (Fasman, 1979; Tatchell & Van Holde, 1979), the complex superhelix–helix transition is likely due to both the nucleosomes and the polynucleosome structure previously detected in similar unsheared chromatin (Finch & Klug, 1976; Nicolini & Kendall, 1977). CD spectra temperature profiles of native unsheared chromatin can then be used to study the stabilization of both the secondary (B-form DNA) and tertiary–quanternary (nucleosome–polynucleosome) structures (Fasman, 1979; Wilhelm, 1974; Nicolini, 1979).

(C) Differences in the Thermal Stability of Higher Order DNA Superstructures in Native G_1- and S-Phase Chromatin. A comparison of the positive components of the chromatin $d[\Theta_{276}]/dT$ vs. T profiles in Figure 1b indicates that, at temperatures lower than T_m, there are many fluctuations in the rate of increase of native G_1-phase chromatin $[\Theta_{276}]$ between 46 and 89 °C, with the highest rates of increase occurring between 65 and 80 °C. In contrast, there are fewer fluctuations in the rate of increase of native S-phase chromatin $[\Theta_{276}]$ over a narrower temperature interval (48–71 °C), and the highest rates of increase are observed at temperatures between 55 and 70 °C.

It can be inferred from these observations and data in the preceding sections of these Results that differences in these patterns of increase in $[\Theta_{276}]$, seen during the thermal denaturation of native chromatins, probably reflect the disruption of different types of low $[\Theta_{276}]$ DNA organizations which are maintained by DNA–protein interactions. This inference has been previously justified and is supported also by the following considerations.

(a) It was shown in Figure 1 and Table I that native proteins maintain inherently high $[\Theta_{276}]$ DNA molecules in lower $[\Theta_{276}]$ configurations in native chromatin. They produce this effect either by shielding asymmetric DNA chromophores or by organizing these chromophores into configurations which tend to cancel asymmetric optical signals.

(b) By definition, changes in positive values of $d[\Theta_{276}]/dT$ reflect changes in the rates of appearance of optically asymmetric DNA chromophores.

(c) Fluctuations in positive values of $d[\Theta_{276}]/dT$ during thermal denaturation must, therefore, reflect fluctuations in the rate of disruption of the DNA–protein interactions that maintain DNA in low $[\Theta_{276}]$ configurations.

It seems reasonable to conclude from these considerations that changes in the rate of increase in native chromatin $[\Theta_{276}]$ seen in Figure 1 are principally due to the progressive dis-

ruption of differentially stable families of nucleosomal and polynucleosomal nucleoprotein superstructures which melt at temperatures lower than T_m.

The fact that in the superhelix–helix transition of unsheared chromatin we may have a contribution also from a polynucleosomal "quaternary" structure (Nicolini, 1979; Nicolini & Kendall, 1977; Finch & Klug, 1976) is suggested also by the following considerations.

(a) The existence of such polynucleosomal superstructures in native unsheared chromatin has recently been indicated by independent and parallel spectroscopic (Nicolini et al., 1976; Nicolini & Kendall, 1977; Nicolini, 1979), electron microscopy (Finch & Klug, 1976; Basu, 1979), and X-ray diffraction (Sperling & Klug, 1977) studies.

(b) While nucleosome can be properly reconstituted from its basic native constituents (Tatchell & Van Holde, 1979), this does *not* occur for the native chromatin here discussed when reconstituted with its original amount of DNA, HAP, and NHAP (see Table I).

(c) Sheared chromatin, which has lost the native polynucleosomal superstructure (Nicolini et al., 1976; Finch & Klug, 1976) and consists of nucleosome filament (Sperling & Klug, 1977), displays both quite a larger $[\Theta_{272}]^{27°C}$ (Nicolini et al., 1976) and a smaller increase in molar ellipticity during the first thermal transition prior to helix–coil transition (Miller et al., 1976) in respect to native unsheared chromatin analyzed here. We would like to stress, however, that the specific findings and data presented in this paper cannot positively discriminate between contributions due either to nucleosome alone or to both nucleosome and polynucleosome "supercoil" combined. Therefore, we will generally refer mainly to chromatin superstructure in discussing the first thermal transition.

To simplify subsequent quantitative comparisons of the thermal stabilities of these low $[\Theta_{276}]$ superstructures in native and reconstituted nucleoproteins, we shall use the derived characterization parameter $\Delta[\Theta_{276}]/\Delta T$. This parameter is a measure of the difference between $[\Theta_{276}]^{max}$ and $[\Theta_{276}]^{27°C}$ divided by the temperature interval ΔT ($T_{\theta^{max}} - T_{\theta^{initial}}$) over which these increases in $[\Theta_{276}]$ are observed. Thus a chromatin preparation having a low $\Delta[\Theta_{276}]/\Delta T$ has its DNA packaged into families of superstructures whose relative overall thermal stabilities are greater than a chromatin preparation having a higher $\Delta[\Theta_{276}]/\Delta T$.

Data in Figure 1 and in Table I show that the $\Delta[\Theta_{276}]/\Delta T$ of G_1 chromatin (74 (deg cm^2/dmol)/°C) is significantly lower than the $\Delta[\Theta_{276}]/\Delta T$ of S-phase chromatin (89 (deg cm^2/dmol)/°C) and suggest that compact, low $[\Theta_{276}]^{27°C}$ DNA superstructures in native G_1-phase chromatin are more thermally stable than disperse, higher $[\Theta_{276}]$ organizations within superstructures found in native S-phase chromatin.

(2) Physical Properties of Nucleohistones Formed by Reconstitution of G_1- or S-Phase HAP Histone Fractions with High Molecular Weight DNA: $G_1(H)$ and $S(H)$. To help determine how components found in histone and NHCP fractions of G_1- and S-phase chromatin affect the physical structure and thermal stability of native and reconstituted nucleoprotein complexes and to provide a perspective from which the preceding results could be analyzed, high molecular weight log-phase HeLa DNA was reconstituted with either G_1- or S-phase HAP histone fractions as described under Methods and in Table II. The $[\Theta_{276}]$ of these nucleohistones were measured during thermal denaturation, and $d[\Theta_{276}]/dT$ vs. T, $\Delta[\Theta_{276}]$, T_m, and ΔT were determined. It can be seen

Table II: Absorbance Ratios of G_1- and S-Phase Histone and Nonhistone Chromosomal Proteins to DNA Determined by Spectrophotometric Analysis[a]

nucleoprotein	HAP histones	HAP non-histones	total protein
G_1 native	0.96	0.46	1.42
S native	0.99	0.48	1.47
$G_1(H)G_1(NH)$	0.96	0.46	1.42
S(H)S(NH)	0.99	0.48	1.47
$G_1(H)S(NH)$	0.98	0.48	1.46
$S(H)G_1(NH)$	0.95	0.47	1.42
$G_1(H)$	0.95		0.95
S(H)	0.99		0.99

[a] Reconstituted nucleoproteins were formed by NaCl–urea gradient analysis of high molecular weight log-phase DNA with either G_1- or S-phase histones with or without nonhistone proteins isolated from hydroxylapatite column. The histone and nonhistone mass proportions to DNA used during gradient dialysis reconstitutions are shown in the table. DNA was determined by its absorbance at 260 nm by use of the molar extinction coefficient of 6226 and mean nucleotide weight of 330. The absorbance at 280 nm of 1.0 mg/mL of purified HeLa S-3 histones in dissociating buffer equals 1.05. Nonhistone proteins were estimated by their absorbance at 280 nm in dissociation buffer with reference to 1.0 mg/mL of BSA = 1.03 A_{280} under the same conditions. $G_1(H)S(NH)$ represents the reconstitution of G_1-phase histones and S-phase nonhistones with log-phase DNA by NaCl-urea gradient dialysis. Similar coding is used for other reconstitutions.

in Table I that G_1- and S-phase HAP histone fractions interacting with high molecular weight DNA during reconstitution have the capacity to produce nucleohistone complexes whose physical properties are in some ways similar to the native G_1- and S-phase chromatin but are paradoxically reversed. Specifically, when the S-phase HAP histone fraction is reconstituted with DNA, its $[\Theta_{276}]^{27°C}$ (3754 deg cm^2/dmol) and T_m (86 °C) are somewhat comparable to the $[\Theta_{276}]^{27°C}$ (3800 deg cm^2/dmol) and T_m (92 °C) of native G_1-phase chromatin. When the G_1-phase HAP histone fraction is reconstituted with DNA, its $[\Theta_{276}]^{27°C}$ (5087 deg cm^2/dmol), $T_{\theta^{max}}$ (72°C), and T_m (80 °C) are very similar to native S-phase chromatin $[\Theta_{276}]^{27°C}$ (5106 deg cm^2/dmol), $T_{\theta^{max}}$ (71 °C), and T_m (82 °C). These data, together with the observed similarity of $T_{\theta^{max}}$ and T_m in reconstituted G_1-phase nucleohistone and native S-phase chromatin (Table I), indicate that during in vitro reconstitution, components found in the HAP G_1-phase histone fraction have the capacity to produce a structure which approaches the properties of native S-phase chromatin during thermal denaturation (lower T_m, higher $\Delta[\Theta_{276}]/\Delta T$).

In vitro reconstitution of S-phase HAP histone with high molecular weight DNA produces an apparently compact nucleohistone whose initial molar ellipticity $[\Theta_{276}]^{27°C}$ (3754 deg cm^2/dmol) is very similar to the $[\Theta_{276}]^{27°C}$ of native G_1-phase chromatin (3800 deg cm^2/dmol). However, during thermal denaturation, the amount of apparent superhelical organization sensitive to disruption by heating to $T_{\theta^{max}}$ ($\Delta[\Theta_{276}]$ = 3777 deg cm^2/dmol) found in reconstituted S-phase nucleohistone is greater than that found in native G_1-phase chromatin ($\Delta[\Theta_{276}]$ = 3180 deg cm^2/dmol).

These data suggest that, during reconstituion in vitro, components found in the S-phase HAP histone fraction have the capacity to produce a structure whose initial molar ellipticity is paradoxically similar to native G_1-phase chromatin. However, during thermal denaturation it is evident that the structure of S-phase nucleohistone is more unstable than native G_1-phase chromatin ($T_{\theta^{max}}$ and the T_m are significantly less

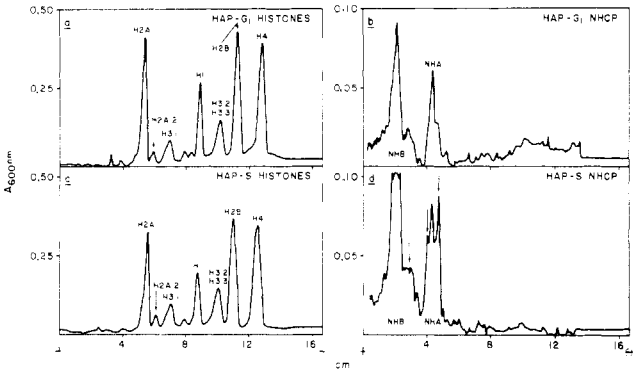

FIGURE 2: Absorbance profiles at 600 nm of histone and nonhistone chromosomal protein fractions resolved at 16 cm, 12% polyacrylamide slab gels containing Triton X-100. Protein fractions were prepared and electrophoresed as described under Methods. (a) Thirty micrograms of HAP isolated G_1-phase histone fractions; (b) 12 μg of HAP isolated G_1-phase nonhistone fraction; (c) 30 μg of HAP isolated S-phase histone fraction; (d) 12 μg of HAP isolated S-phase nonhistone fractions.

and $\Delta[\Theta_{276}]/\Delta T$ is greater than that observed with native G_1-phase chromatin).

These puzzling results led us to investigate the composition of HAP histone and NHCP fractions of G_1- and S-phase HeLa cells by use of electrophoresis on polyacrylamide gels containing Triton X-100 (Zweidler & Cohen, 1972).

(*3*) *Purity of HAP Histone and NHCP Fractions.* Equivalent quantities of native G_1- and S-phase chromatin were fractionated by chromatography on HAP as described in section e of Methods. HAP histone and NHCP fractions were then resolved by electrophoresis on 12% polyacrylamide slab gels containing 6 mM Triton X-100 and 6 M urea as described in section f of Methods. The following can be seen in Figure 2.

(a) All principal and minor histone classes are recovered in HAP histone fractions and have similar relative proportions in G_1- and S-phase chromatin (Figures 2a, c).

(b) HAP NHCP fractions contain two principal groups of proteins when resolved by electrophoresis under these conditions. A comparison of the profiles in Figures 2b,d indicates that the S-phase NHCP fraction contains more components (arrows) in both groups.

(c) G_1- and S-phase histone and nonhistone fractions eluted from HAP appear to be essentially free of cross-contaminating protein species (compare Figures 2a and 2c with 2b and 2d). Furthermore, purified histone H1 was subjected to chromatography on HAP, and it was found that 99% of the A_{280} applied to the column was eluted in the HAP histone fraction (i.e., in 1 mM sodium phosphate, 4 M urea, 2 M NaCl, 1 mM DTT, 0.1 mM PMSF, pH 6.0).

(*4*) *Analysis of Histone Phosphorylation and Acetylation Levels During the HeLa S-3 Cell Cycle.* Since the data in the preceding section indicate that HAP histone fractions in fact essentially contain only histones, we wished to determine what difference between G_1- and S-phase histones could be responsible for the strikingly different nucleohistone reconstitution products observed in section 2c of these Results.

After identifying the positions of phosphorylated and acetylated histone species on acid–urea gels containing Triton X-100 (see Methods, section g), histones were extracted from synchronized HeLa cells at various stages of the cell cycle, and relative levels of nucleosomal histone phosphorylation and acetylation at different stages of the cell cycle were determined as described under Methods (section g). Various phosphorylated and acetylated histone H2A, H2B, H3, and H4 species

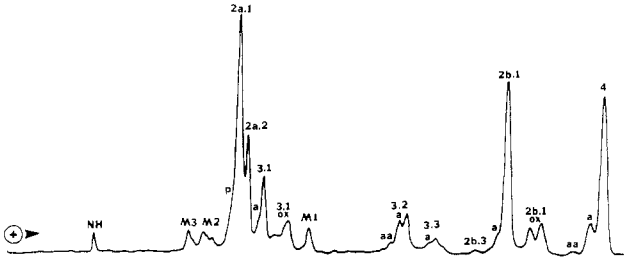

FIGURE 3: Histones of S-phase HeLa cells (12 h after mitotic selection) from which H1 had been removed by extraction with 5% trichloroacetic acid were electrophoresed for 24 h at 200 V on 28 × 0.4 cm 12% polyacrylamide gels containing 6 M urea and 6 mM Triton X-100. The gel was stained with Amido Black and scanned at 650 nm with a Gilson MUV-RP spectrophotometer. 2a, 2b, 3, and 4 = major histone classes; 0.1, 0.2, and 0.3 = primary structure variants of the respective histone classes; M1, M2, and M3 = minor histone species; NH = nonhistone protein; a = acetylated; aa = diacetylated; p = phosphorylated; ox = forms with oxidized methionine residues (Zweidler, 1978).

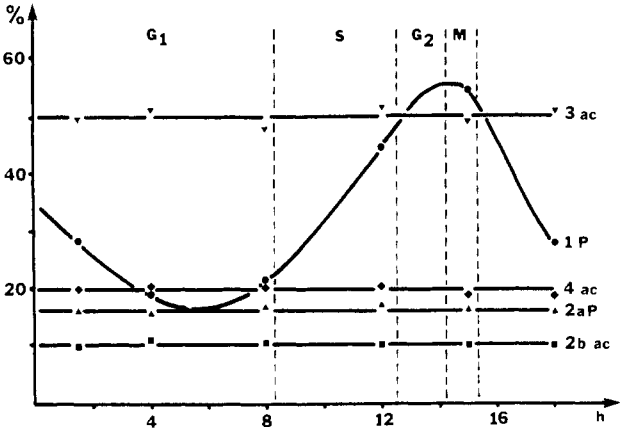

FIGURE 4: Fraction of each histone class which is modified by acetylation (ac) or phosphorylation (p) at different stages of the cell cycle of synchronized HeLa cells, as determined after we resolved and scanned the histones on 28-cm polyacrylamide gels as shown in Figure 5. Major histones H2a, H2b, H3, H4, and H1 are indicated by their terminal numerical codes. Ac represents total acetate and P, total phosphate.

present in S-phase HeLa histone fractions are indicated in Figure 3. In Figure 4, it can be seen that, throughout the HeLa S-3 cell cycle from G_1 through G_2 phase, relative levels of nucleosomal core histone acetylation or phosphorylation do not change significantly. Thus, these data demonstrate that there is no appreciable change in the relative amounts of various acetylated or phosphorylated histone H2A, H2B, H3, or H4 species as HeLa cells proceed from G_1 into S phase.

In contrast to these constant levels of modification observed in nucleosomal core histones, it has been previously shown that HeLa histone H1 phosphorylation levels are lower in G_1 than in S phase (Marks et al., 1973). This can also be seen in Figure 4, which demonstrates that, of all the histone modifications observed in this study, only histone H1 phosphorylation levels change during the G_1–S transition in HeLa cells. Figure 5 shows the electrophoretic resolution of G_1- and S-phase histones H1A and H1B which were prepared and analyzed as described by Ajiro et al. (K. Ajiro, A. Zweidler, and T. Borun, unpublished experiments). While a complete discussion of changes in histone H1 phosphorylation levels during the HeLa cell cycle is outside the scope of this paper and is treated elsewhere (K. Ajiro, A. Zweidler, and T. Borun, unpublished experiments), it can be seen from Figure 5 that during the G_1–S transition H1A is transformed from mostly

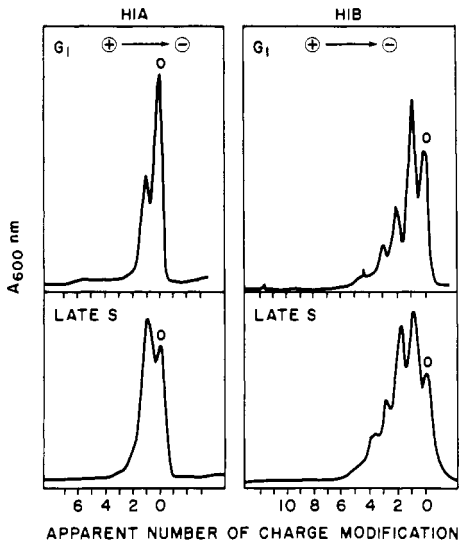

FIGURE 5: Resolution of histone H1A and H1B from G_1- and S-phase HeLa S-3 cells by electrophoresis in 28-cm long acid–urea gels in 1.8-mm diameter tubes. H1A and H1B extracted from G_1- and S-phase cells and resolved by chromatography on 40 × 0.6 cm Amberlite CG-50 columns as described under the Methods of L. H. Cohen, K. Ajiro, and T. W. Borun (unpublished experiments). After we empirically determined the optimal amount of each sample producing best resolution during electrophoresis, 0.50 μg of H1A and 0.25 μg of H1B from G_1-phase cells, 2 μg of H1A and H1B from S-phase cells was resolved by electrophoresis on 28-cm long × 1.8-mm diameter acid–urea polyacrylamide gels for 16 h at 500 V as described in L. H. Cohen, K. Ajiro, and T. W. Borun (unpublished experiments). The marker protein in these gels was 0.2 μg of sea urchin (*S. purpuratus blastula*) H1 mixed with the HeLa H1 fractions just prior to electrophoresis. After staining with Coomassie blue and destaining, we scanned the gels at 550 nm by use of a Gilford spectrophotometer.

unphosphorylated species to mostly mono- and diphosphorylated species. In contrast, H1B is mostly monophosphorylated in the G_1 phase and during the S phase becomes di-, tri-, and tetraphosphorylated. Because bisulfite was not included during extraction of H1 during mitosis in the experiment of Figure 4, differences between the high mitotic H1 phosphorylation level and the lower S-phase level of phosphorylation are underestimated (K. Ajiro, A. Zweidler, and T. Borun, unpublished experiments). For a more complete discussion of H1 phosphorylation in mitosis in mammalian and nonmammalian systems see Gurley et al. (1978) and Ruttle et al. (1979).

It is evident from these data that the only difference between components found in HAP G_1- and S-phase histone fractions which are detectable by the methods used in the present study are differences in levels of H1 phosphorylation. It should be pointed out, however, that, while relative levels of nucleosomal core histone modification do not change during G_1–S transition, it is conceivable that sites of modification do change.

(*5*) *Molar Ellipticity of Reconstituted Chromatins during Thermal Denaturation.* To help determine how changes in the composition of histone and NHCP fractions are related to increases in native chromatin molar ellipticity and decreases in chromatin thermal stability as HeLa cells proceed from G_1 into S phase we examined the molar ellipticity of reconstituted nucleoproteins during thermal denaturation. HAP histone RNA-free NHCP fractions of G_1- and S-phase chromatin were isolated and reconstituted with high molecular weight log-phase HeLa DNA by NaCl–urea gradient dialysis as described under Methods and in Table II. After reconstitution, we determined the $[\Theta_{276}]^{27°C}$, $\Delta[\Theta_{276}]/\Delta T$, and T_m of these preparations during thermal denaturation from 27 to 92 °C (Table I).

For the homologous reconstitution $[G_1(H)G_1(NH)]$ and $[S(H)S(NH)]$ the large physical differences between native G_1- and S-phase chromatin are not found in reconstituted G_1- and S-phase chromatin. Thus, $[\Theta_{276}]^{27°C}$, T_m, and $\Delta[\Theta_{276}]/\Delta T$ are reversed in reconstituted G_1- and S-phase chromatin, when compared to their respective native chromatins. Heterologous reconstitutions (see Table I) of hybrid (G_1–S)-phase nucleoproteins show that mixed reconstitutions of NHCP and of HAP protein fractions from G_1- and S-phase chromatin with high molecular weight log-phase HeLa DNA chromatins are obtained whose physical properties appear to be generally quite similar ($[\Theta_{276}]^{27°C}$, T_m, and ΔT). Despite the preceding similarities, however, $[G_1(H)S(NH)]$ has a $[\Theta_{276}]$ (3597 deg cm^2/dmol) and $\Delta[\Theta_{276}]/\Delta T$ of 156 (deg cm^2/dmol)/°C which is significantly less than the $[\Theta_{276}]$ and $\Delta[\Theta_{276}]/\Delta T$ of reconstituted chromatin containing $[S(H)G(NH)]$ (4836 deg cm^2/dmol and 210 (deg cm^2/dmol)/°C, respectively). Thus, $[G_1(H)S(NH)]$ higher order nucleoprotein structures appear to be more stable than $[S(H)G_1(NH)]$ superstructures while the DNA helix stabilities (T_m) are similar.

Discussion

(*A*) *Relationship of Molar Ellipticity to Native Chromatin Superpacking and Histone H1 Phosphorylation.* It should be emphasized at the outset of this discussion that molar ellipticity at 276 nm is merely a measure of the net chiral asymmetry of DNA chromophores under standarized conditions (see Methods, section i). Thus, while a more *optically* active (asymmetric) arrangement of DNA chromophores will by definition have a higher $[\Theta_{276}]^{27°C}$, the relationship between a given value of $[\Theta_{276}]^{27°C}$ and specific *physical* arrangements of chiral DNA chromophores in either isolated DNA in solution or in nucleoprotein complexes is obscure. However, in preliminary studies, it has been possible to empirically demonstrate that the magnitudes of the $[\Theta_{276}]^{27°C}$ value found in native G_1- and S-phase chromatin do in fact represent specific structural arrangements of DNA–protein complexes in HeLa cells in situ.

(1) Isolated G_1- and S-phase HeLa DNA both have similar high values of $[\Theta_{276}]^{27°C}$, indicating that the chiral chromophores of both of these protein-free DNAs exist in solution in configurations which are similar and have highly asymmetric optical properties.

(2) Native G_1-phase chromatin has a low $[\Theta_{276}]^{27°C}$, indicating that the chiral chromophores of DNA in G_1-phase chromatin have been organized into structures which are less optically active than free DNA. Independent measurements have correlated these low $[\Theta_{276}]^{27°C}$ configurations of native HeLa G_1-phase chromatin DNA with (a) the absence of DNA replication in vivo (Nicolini et al., 1975), (b) physically compact configurations of chromatin DNA in situ (Kendall et al., 1977), (c) low levels of histone H1 phosphorylation in vivo (Marks et al., 1973; K. Ajiro, A. Zweidler, and T. Borun, unpublished experiments), (d) fewer actinomycin D (Pederson, 1972) and ethidium bromide binding sites than are detectable in protein-free DNA or native S-phase chromatin (Nicolini et al., 1975), and (e) high levels of differential light scattering [Nicolini, 1979, and Table I].

All of these data taken together coherently suggest that the DNA in native G_1-phase chromatin is physically organized into compact polynucleosomal structures (like a supercoil) whose relatively low $[\Theta_{276}]^{27°C}$ probably reflects a relatively high degree of physical superpacking (supercoiling). The existence of polynucleosomal superstructures in native unsheared chromatin has been recently suggested by parallel spectroscopic (Nicolini et al., 1976; Nicolini & Kendall, 1977;

Nicolini, 1979), electron microscopy (Finch & Klug, 1976; Basu, 1979), and X-ray diffraction (Sperling & Klug, 1977) studies. Furthermore, these putative polynucleosomal superstructures do not replicate in vivo but do support RNA transcription.

(3) Native S-phase chromatin has a moderately high $[\Theta_{276}]^{27°C}$, indicating that as HeLa cells proceed from G_1 into S phase, the low $[\Theta_{276}]^{27°C}$ DNA configurations in G_1 phase chromatin are reorganized into more optically asymmetric S-phase configurations. Independent measurements have correlated the more asymmetric configurations of native HeLa S phase chromatin DNA with (a) DNA replication in vivo (Nicolini et al., 1975), (b) physically disperse chromatin DNA configurations in situ (Kendall et al., 1977), (c) higher levels of histone H1 phosphorylation in vivo (Marks et al., 1973; K. Ajiro, A. Zweidler, and T. Borun, unpublished experiments), (d) more actinomycin D (Pederson, 1972) and ethidium bromide binding sites than are detectable in native G_1-phase chromatin but less binding sites than in protein-free DNA (Nicolini et al., 1975), and (e) lower levels of differential light scattering (Nicolini, 1979, and Table I).

From these observations it seems probable that the optically asymmetric configurations of DNA in S-phase chromatin correspond to physically dispersed polynucleosomal structures which are in the process of being replicated and transcribed in vivo.

(4) The $[\Theta_{276}]^{27°C}$ of HeLa chromatin isolated from highly condensed (Kendall et al., 1977) and physically very supercoiled mitotic chromosomes is even lower (2400 deg cm^2/dmol) (Nicolini et al., 1975) than the $[\Theta_{276}]^{27°C}$ of native G_1-phase chromatin (3800 deg cm^2/dmol; Table I), demonstrating that there is a relatively straightforward correlation between low values of $[\Theta_{276}]^{27°C}$ and high levels of native chromatin superpacking into putative supercoiled structures throughout the HeLa cell cycle.

In all the native and reconstituted nucleoproteins examined in the present study, molar ellipticity at 276 nm increases as the temperature is raised during thermal denaturation, at least until significant DNA melting occurs to produce negative signals. Protein-free DNA, "poorly" reconstituted chromatin, chromatin treated with 1% sodium dodecyl sulfate, and chromosomal RNA alone (data not shown) do not exhibit increases in $[\Theta_{276}]$ during thermal denaturation under the low ionic strength conditions used in the present study. It is thus probable that these increases in chromatin $[\Theta_{276}]$ reflect a rearrangement of less optically active, physically superpacked DNA components into more optically active configurations as protein components of the nucleoprotein, which stabilize the superpacked DNA, become partially dissociated from the DNA or rearrange the DNA during thermal denaturation. The temperature at which $d[\Theta_{276}]/dT$ reaches its maximum positive value is, by definition, the temperature at which all reactions resulting in a net increase in the optical asymmetry of DNA chromophores reach their net maximum rate during the course of thermal denaturation. If DNA superstructures are stabilized by a number of different proteins or by the same type of protein in different configurations which have different thermal stabilities, it is evident that the melting of superpacked DNA organizations would be a very complex phenomenon. It can be seen in Figure 1b that profiles of nucleoprotein $d[\Theta_{276}]/dT$ vs. T during thermal denaturation are in fact complex. Thus, the present data suggest a possible functional interrelationship among higher order families of DNA superstructures with differential thermal stabilities, localized regions of gene transcription, or DNA replication and families of differentially phosphorylated H1A and H1B molecules in G_1- and S-phase HeLa S-3 cells.

(*B*) *Relationship of Histone H1 Phosphorylation Levels to the Molar Ellipticity and Thermal Stability of Reconstituted Nucleoproteins.* It was shown in section 2 of the Results that the $[\Theta_{276}]^{27°C}$ of reconstituted G_1-phase nucleohistones was paradoxically high, similar to that of native S-phase chromatin, and that the $[\Theta_{276}]^{27°C}$ of reconstituted S-phase nucleohistone was paradoxically low, similar to that of native G_1-phase chromatin. The only other difference detected between the G_1- and S-phase HAP histone fractions, among several parameters examined, was in the levels of histone H1 phosphorylation.

These results suggest that the differences in H1 phosphorylation levels found in G_1- and S-phase HeLa cells are responsible for the two radically different nucleohistone structures formed when histones of these stages are recombined with DNA by NaCl–urea gradient dialysis. It is easy to understand how the level of H1 phosphorylation might be important in the reconstitution of compact nucleohistone structures. Phosphorylations of H1 undoubtedly decrease the tightness of associations of the molecule with DNA (a single phosphate group increases the elution rate of H1 from ion-exchange resins) and thus should allow better annealing of disordered or random arrangements of H1 and histones established during the early part of the reconstitution experiments. Such disordered associations are particularly serious since H1 reacts faster than nucleosomal histones in binding DNA under in vitro dialysis conditions (Kleiman & Huang, 1972; Chae, 1975). Other studies (Adler et al., 1972) have shown that, in the absence of nucleosomal core histones, less phosphorylated H1 produced less optically active H1–DNA complexes than do more phosphorylated H1 molecules. Thus the physical properties manifested by both native and reconstituted chromatins during thermal denaturation imply H1 plays a predominant role in the superstructural organization with NHCP acting cooperatively with H1 in a fashion not yet understood.

(*C*) *Effects of G_1- and S-Phase HAP NHCP on the Apparent Physical Properties of Reconstituted Nucleoproteins (Table I).* It can be inferred from the data in Table I that G_1(NH) and S(NH) both facilitate the formation of compact, low $[\Theta_{276}]^{27°C}$ nucleoproteins when compared to G_1(H). This nonhistone protein effect may be due to the reduction of preliminary G_1-phase histone H1–DNA interaction during gradient dialysis, allowing for a relatively higher degree of supercoiling than when this nonhistone protein competition is absent in G_1(H). Both of these nonhistone fractions appear to increase the thermal stability of the high level of putative superhelical organization which they induce when reconstituted with G_1(H) and DNA (i.e., both nonhistone fractions increase $T_{\Theta^{max}}$). However, S(NH) is apparently able to allow for more superhelical organization of G_1(H)S(NH) chromatin (lower $[\Theta_{276}]^{27°C}$, higher $\Delta[\Theta_{276}]$) but is not as efficient in stabilizing these superstructures against thermal denaturation (higher $\Delta[\Theta_{276}]/\Delta T$) than G_1(NH). On the other hand the inclusion of either G_1(NH) or S(NH) with S(H) and DNA during gradient dialysis gives rise to nucleoprotein products which are in both cases more compact with more putative high-order structures (lower $[\Theta_{276}]^{27°C}$). S-phase NHCP appear to promote the formation of more stable higher order structures but less-stable structures stabilizing the DNA helix against thermal denaturation (higher $T_{\Theta^{max}}$, lower $\Delta[\Theta_{276}]/\Delta T$ but lower T_m) than G_1-phase NHCP. Thus it follows that those nonhistone interactions contributing to the formation and

stabilization of higher order structures in reconstituted chromatin can be different from those contributing to double-helical DNA stability. Also the degree of compaction or superstructural organization is also independent of the stability of these supercoiled structures in that S(H)G_1(NH) forms more compact (lower $[\Theta_{276}]^{27°C}$) but less stable structures (lower $T_{\Theta max}$, higher $\Delta[\Theta_{276}]/\Delta T$) than S(H)S(NH) reconstituted chromatin. In conclusion, it is probable that both S-phase and G_1-phase NHCP allow for the low $[\Theta_{276}]^{27°C}$, compact structures by reducing S-phase H1–DNA interactions somewhat during reconstitution to produce products whose $[\Theta_{276}]^{27°C}$ values are slightly lower than for S-phase nucleohistone alone. In addition, G_1-phase nonhistones seem to be more effective in reducing these S-phase H1–DNA interactions during reconstitution since S(H)G_1(NH) has a lower $[\Theta_{276}]^{27°C}$ than S(H)S(NH).

The observations in this paper are of interest for several reasons. First, they introduce and coherently support the general concept that in vitro interactions among histone H1 molecules, DNA, and NHCP are responsible for the formation of reconstituted chromatins whose superstructural organizations are significantly different from those found in native chromatins or those produced during the reconstitution of nucleohistones. Second, they indicate that changes in H1–DNA–NHCP interactions occur in vivo, are modulated by H1 phosphorylation, and appear responsible for the relaxation of G_1-phase superstructures into S-phase configurations during the HeLa S-3 cell cycle. Third, they help delineate how histone H1 phosphorylation could function together with NHCP in the regulation of DNA replication and transcription.

References

Adler, A. J., Langan, T. H., & Fasman, C. D. (1972) *Arch. Biochem. Biophys. 153*, 769–777.

Ansevin, A. T., Vizaro, D. L., Brown, B. W., & McConthy, J. (1976) *Biopolymers 15*, 153–174.

Augenlicht, L., Nicolini, C., & Baserga, R. (1974) *Biochem. Biophys. Res. Commun. 59*, 920–926.

Baserga, R., & Nicolini, C. (1976) *Biochim. Biophys. Acta 458*, 109–134.

Basu, S. (1979) in *Chromatin Structure and Function* (C. Nicolini, Ed.) Vol. II, pp 515–540, Plenum Press, New York.

Bayley, P. M. (1973) *Prog. Biophys. Mol. Biol. 27*, 1–76.

Borun, T. W., Gabrielli, F., Ajiro, K., Zweidler, A., & Baglioni, C. (1975) *Cell 4*, 59–67.

Borun, T. W., Ajiro, K., Zweidler, A., Dolby, T. W., & Stephens, R. E. (1977) *J. Biol. Chem. 252*, 173–180.

Cech, C. L., Hug, W., & Tinoco, I. (1976) *Biopolymers 15*, 131–152.

Chae, C. (1975) *Biochemistry 14*, 900–906.

Cox, R., Damjanov, I., Abanobi, S. E., & Sarma, D. S. R. (1973) *Cancer Res. 33*, 2114–2121.

Eijher, J., Schildkraut, C., & Doty, P. (1962) *Biochim. Biophys. Acta 55*, 13–19.

Fasman, G. (1979) in *Chromatin Structure and Function* (C. Nicolini, Ed.) Vol. I, pp 67–108, Plenum Press, New York.

Fasman, G. D., Lindblow, C., & Grossman, L. (1964) *Biochemistry 3*, 1015–1021.

Finch, J. F., & Klug, A. (1976) *Proc. Natl. Acad. Sci. U.S.A. 73*, 1897–1901.

Garel, A., Zolan, M., & Axel, R. (1977) *Proc. Natl. Acad. Sci. U.S.A. 74*, 4867–4871.

Gilmour, R. S., Windass, J. D., Affara, N., & Paul, J. (1975) *J. Cell. Physiol. 85*, 449–458.

Gottesfeld, J. M., Murphy, R. F., & Bonner, J. (1975) *Proc. Natl. Acad. Sci. U.S.A. 72*, 4404–4408.

Gross-Bellard, M., Oudet, P., & Chambon, P. (1973) *Eur. J. Biochem. 36*, 32–38.

Gurley, L. R., D'Anna, J. A., Barham, S. S., Daven, L. L., & Tobey, R. E. (1978) *Eur. J. Biochem. 84*, 1–15.

Kendall, F., Swenson, R., Borun, T., Rowinski, J., & Nicolini, C. (1977) *Science 196*, 1106–1109.

Kleiman, L., & Huang, R. C. (1972) *J. Mol. Biol. 64*, 1–8.

Kornberg, R. D. (1977) *Annu. Rev. Biochem. 46*, 931–954.

MacGillivray, A. J., Cameron, A., Krauze, R. J., Rickwood, D., & Paul, J. (1972) *Biochim. Biophys. Acta 277*, 384–402.

Mandel, R., & Fasman, C. D. (1974) *Biochem. Biophys. Res. Commun. 59*, 672–679.

Mandel, R., & Fasman, G. D. (1976) *Biochemistry 15*, 3122–3130.

Marks, D. B., Paik, W. K., & Borun, T. W. (1973) *J. Biol. Chem. 248*, 5660–5667.

Milgram, E. (1975) Internal Report No. 8/75, Division of Biophysics, Temple University, Philadelphia, PA.

Miller, P., Kendall, F., & Nicolini, C. (1976) *Nucleic Acids Res. 3*, 1875–1881.

Nicolini, C. (1979) in *Chromatin Structure and Function* (C. Nicolini, Ed.) Vol. II, pp 613–667, Plenum Press, New York.

Nicolini, C., & Baserga, R. (1975) *Chem.-Biol. Interact. 11*, 101–116.

Nicolini, C., & Kendall, F. (1977) *Phys. Chem. Phys. 9*, 265–283.

Nicolini, C., Ajiro, K., Borun, T. W., & Baserga, R. (1975) *J. Biol. Chem. 250*, 3381–3385.

Nicolini, C., Baserga, R., & Kendall, F. (1976) *Science 192*, 796–798.

Olins, A. L., & Olins, D. E. (1974) *Science 183*, 330–332.

Ormerod, M. D., & Lehmann, A. R. (1971) *Biochim. Biophys. Acta 247*, 369–372.

Oudet, P., Gross-Bellard, M., & Chambon, P. (1975) *Cell 4*, 281–299.

Parodi, S., Mulivor, R. A., Martin, J. T., Nicolini, C., Sarma, D. S. R., & Farber, E. (1975) *Biochim. Biophys. Acta 407*, 174–190.

Pederson, T. (1972) *Proc. Natl. Acad. Sci. U.S.A. 69*, 2224–2228.

Polacow, I., & Simpson, R. T. (1973) *Biochem. Biophys. Res. Commun. 52*, 202–207.

Rao, P., Wilson, B., & Puck, T. T. (1976) *J. Cell. Physiol. 91*, 131–142.

Robbins, E., & Marcus, P. I. (1964) *Science 144*, 1152–1153.

Rattle, H., Baldwin, H., Cary, P., Swan, P., & Bradbury, E. (1979) in *Chromatin Structure and Function* (C. Nicolini, Ed.) Vol. II, pp 451–514, Plenum Press, New York.

Seligy, V. L., & Lurquin, P. F. (1973) *Nature (London), New Biol. 243*, 20–21.

Shih, T. Y., & Fasman, G. D. (1972) *Biochemistry 11*, 398–404.

Spelsberg, T. C., Hnilica, L. S., & Ansevin, A. T. (1971) *Biochim. Biophys. Acta 228*, 550–562.

Sperling, A., & Klug, A. (1977) *J. Mol. Biol. 112*, 253–263.

Tashiro, T., & Kurokawa, M. (1975) *Eur. J. Biochem. 60*, 569–577.

Tatchell, K., & Van Holde, K. E. (1979) in *Chromatin Structure and Function* (C. Nicolini, Ed.) Vol. II, pp 413–426, Plenum Press, New York.

Terasima, T., & Tolmach, L. J. (1963) *Exp. Cell Res. 30*, 344–362.

van der Schans, G. P., Aten, J. B. T., & Blok, J. (1969) *Anal. Biochem. 32*, 14–30.
Weintraub, H., & Groudine, M. (1976) *Science 193*, 848–856.
Wilhelm, F. K., deMurcia, G. M., Champagne, M. H., & Duane, M. P. (1974) *Eur. J. Biochem. 45*, 431–443.
Woodcock, C. L. F., Sweetman, H. E., & Frado, L. L. (1976) *Exp. Cell Res. 97*, 111–119.
Zweidler, A. (1978) in *Methods in Chromosomal Protein Research* (Stein, G. S., & Stein, J., Eds.) Academic Press, New York (in press).
Zweidler, A., & Cohen, L. H. (1972) *Fed. Proc., Fed. Am. Soc. Exp. Biol. 31*, 926a.
Zweidler, A., & Borun, T. W. (1974) *J. Cell. Biol., Abstr. 63*, 386a.

Purification and Properties of the σ Subunit of *Escherichia coli* DNA-Dependent RNA Polymerase†

Peter A. Lowe, Dayle A. Hager, and Richard R. Burgess*

ABSTRACT: An improved purification procedure is described for the σ subunit of *Escherichia coli* DNA-dependent RNA polymerase [ribonucleoside triphosphate:RNA nucleotidyltransferase, EC 2.7.7.6]. The method involves chromatography of purified RNA polymerase on single-stranded DNA–agarose, Bio-Rex 70, and finally Ultragel AcA44. The σ factor obtained is electrophoretically pure with a yield of about 40%. A number of the chemical–physical properties of σ are presented. A molecular weight of 82 000 was determined by phosphate buffered sodium dodecyl sulfate–polyacrylamide gel electrophoresis. Ultraviolet absorption spectra were used to determine an $E_{280nm}^{1\%}$ of 8.4. The amino acid composition and 12-residue N-terminal sequence (Met-Glx-Glx-Asx-Pro-Glx-(Ser or Cys)-Glx-Leu-Lys-Leu-Leu) of σ have been determined. The isoelectric focusing properties of σ are presented. Denaturation–renaturation studies indicate that σ is capable of an unusually rapid and complete recovery of activity after being subjected to denaturing conditions. A stable, 40 000-dalton fragment is generated from σ by mild trypsin treatment.

Escherichia coli DNA-dependent RNA polymerase holoenzyme ($\alpha_2\beta\beta'\sigma$) can be reversibly dissociated into a σ subunit and a core polymerase ($\alpha_2\beta\beta'$) (Burgess et al., 1969; Burgess, 1971). The σ subunit is used catalytically and is required for efficient polymerase binding and initiation of RNA synthesis at bacterial and bacteriophage promoters (Travers & Burgess, 1969; Chamberlin, 1976). Recently the location of the σ gene has been determined to be at about 66 min of the *E. coli* genetic map. Nakamura et al. (1977) and Harris et al. (1977) showed that a locus affecting the size of σ mapped in this region. Mutants affecting σ activity map in this region (Gross et al., 1978; Travers et al., 1978; Nakamura, 1978; Harris et al., 1978). Finally, three different mutants of σ have been shown to differ from wild type σ and each other in their tryptic peptide patterns (Burgess, R., Gross, C., and Lowe, P., unpublished observations).

Although several papers dealing with the purification of σ have appeared (Burgess et al., 1969; Burgess & Travers, 1971; Berg et al., 1971; Burgess, 1976), detailed studies of the chemical and physical properties of σ and its role in transcription have been delayed by the difficulty of obtaining milligram amounts of σ with satisfactory purity. We present here the details of a method for obtaining pure σ in amounts to allow its physical and chemical characterization. The purification procedure uses as starting material the RNA polymerase purified by the method of Burgess & Jendrisak (1975) through the Polymin P precipitation, DNA cellulose, and gel filtration chromatography steps. This RNA polymerase does contain minor impurities and is not saturated with σ or free of subassemblies caused by polymerase dissociation. Therefore, we purify it further and resolve it into core polymerase and holoenzyme by stepwise elution from a single-stranded DNA–agarose (Nüsslein & Heyden, 1972). Pure holoenzyme is separated into core polymerase and σ by chromatography on a tandem column of Bio-Rex 70 and DEAE-cellulose. Final purification of σ is achieved by gel filtration chromatography on an Ultragel AcA44 column. The purification scheme presented also includes details for producing highly purified holoenzyme and core polymerase.

We present a number of the chemical and physical properties of σ, including molecular weight, extinction coefficient, absorption spectrum, amino acid analysis, N-terminal sequence, isoelectric focusing characteristics, denaturation–renaturation properties, and proteolytic fragmentation pattern.

Materials and Methods

A. Materials. Guanidine hydrochloride was purchased from Schwarz/Mann and phenylmethanesulfonyl fluoride from Calbiochem. Electrophoresis grade acrylamide, sodium dodecyl sulfate, agarose, *N,N'*-methylenebisacrylamide, *N,N,N',N'*-tetramethylethylenediamine, and ammonium persulfate were obtained from Bio-Rad. Nonidet-P40 was purchased from Gallard-Schlessinger. Urea (technical grade) from Baker was used without further purification. Purified rabbit muscle myosin was a gift from M. Greaser. *E. coli* β-galactosidase, ovalbumin, trypsin, and highly polymerized calf thymus DNA were obtained from Worthington. Bovine serum albumin was purchased from Miles. Beef liver catalase and rabbit muscle phophorylase *a* were obtained from Sigma.

† From the McArdle Laboratory for Cancer Research, University of Wisconsin, Madison, Wisconsin 53706. *Received October 27, 1978; revised manuscript received December 12, 1978.* This paper is in honor of the 70th birthday of Dr. Harold P. Rusch, M.D., founder and long-time director of the McArdle Laboratory for Cancer Research and creator of its productive research atmosphere. This research was supported by NIH Grant CA-07175 and NSF Grant PCM77-25099 (to R.R.B.).

0006-2960/79/0418-1344$01.00/0